

Study of the mass-ratio distribution of spectroscopic binaries. I. A novel algorithm

S. Shahaf,^{*} T. Mazeh, S. Faigler

School of Physics and Astronomy, Tel Aviv University, Tel Aviv 69978, Israel

Accepted 2017 August 30. Received 2017 August 29; in original form 2017 July 12

ABSTRACT

We developed a novel *direct* algorithm to derive the mass-ratio distribution (MRD) of short-period binaries from an observed sample of single-lined spectroscopic binaries (SB1). The algorithm considers a class of parameterized MRDs and finds the set of parameters that best fits the observed sample. The algorithm consists of four parts. First, we define a new observable, the ‘modified mass function’, that can be calculated for each binary in the sample. We show that the distribution of the modified mass function follows the shape of the underlying MRD, turning it more advantageous than the previously used mass function, reduced mass function or reduced mass function logarithm. Second, we derive the likelihood of the sample of modified mass functions to be observed given an assumed MRD. An MCMC search enables the algorithm to find the parameters that best fit the observations. Third, we suggest to express the unknown MRD by a linear combination of a basis of functions that spans the possible MRDs. We suggest two such bases. Fourth, we show how to account for the undetected systems that have an RV amplitude below a certain threshold. Without the correction, this observational bias suppresses the derived MRD for low mass ratios. Numerous simulations show that the algorithm works well with either of the two suggested bases. The four parts of the algorithm are independent, but the combination of the four turn the algorithm to be highly effective in deriving the MRD of the binary population.

Key words: binaries: spectroscopic – methods: statistical – methods: data analysis

1 INTRODUCTION

The study of the mass-ratio distribution (MRD) of binaries, short-period ones in particular, has a long history. This is so because the MRD plays a key role in various aspects of the theory of binary formation and evolution. First, it provides one of the very few ways to confront the theories of binary formation (e.g., Bate & Bonnell 1997; Satsuka et al. 2017) with observations. Second, the primordial MRD is a one of the few major inputs for population syntheses of binaries (e.g., Toonen et al. 2012; Yungelson & Kuranov 2017), which try to predict, for example, the rate of supernova explosion and black hole mergers. Third, the binary fraction and the MRD have been shown to play an important role in star cluster evolution (e.g., Hut et al. 1992; Benacquista & Downing 2013). Finally, understanding the low end of the MRD is crucial for the determination of the borders of the brown dwarf desert (e.g., Mazeh et al. 2003; Grether & Lineweaver 2006) that separates exoplanets from low-mass stellar secondaries.

It is therefore not surprising that quite a few stud-

ies tried to derive the MRD of binaries, using short-period spectroscopic binaries (SB) in particular. Reviews of the early studies can be found in Trimble (1990) and Mazeh & Goldberg (1992). Because some of these studies (e.g., Lucy & Ricco 1979; Duquenois & Mayor 1991; Tokovinin 2000; Goldberg et al. 2003; Fisher et al. 2005; Raghavan et al. 2010; Boffin 2010, 2015; Curé et al. 2015) yielded conflicting results, the shape of the MRD of short-period binaries continues to be an open question.

Derivations of the MRD should be based on a complete sample of binaries discovered by a systematic radial-velocity (RV) search. Generally, MRDs may depend on the mass of the primary star (Kouwenhoven et al. 2009), therefore analyzed samples should be restricted to some narrow range of spectral types. In an ideal world, with spectra of unlimited resolution and signal-to-noise ratio, each SB would be a double-lined binary (SB2), with mass ratio derived directly from the ratio of the RV amplitudes of the two components. In reality, the derivation of the MRD of short-period binaries is based on samples for which most of the binaries observed are single-lined spectroscopic binaries (SB1), where only the RVs of the primary star can be measured. Even after obtaining observations of a large sample of SB1s, de-

* E-mail: sahar@wise.tau.ac.il

iving the MRD is hampered by the fact that for each of the SB1s the orbital solution cannot yield the mass ratio itself but merely the mass function, a combination of two unknowns—the mass ratio and plane-of-motion inclination angle. Therefore, a statistical approach must be applied to the observational results, assuming *random distribution of the orbital inclination* of the sample as a whole.

Two main approaches have been used to disentangle the MRD from the orbital inclination (see, for example, Heacox 1995). In the inverse approach, one considers the sample of derived mass functions and works his/her way back, usually iteratively (see the classical work of Lucy 1974), to the underlying MRD of the binary population (e.g., Lucy & Ricco 1979; Mazeh & Goldberg 1992; Boffin 2010; Curé et al. 2015).

In the direct approach, on the other hand, one assumes a certain MRD of the binary population, calculates the resulting *expected* distribution of some observable, O , and compares it with the set of $\{O_i\}$ obtained from the sample of SB1s, where the i -th binary is represented by O_i . One then finds the MRD that best fits the observed set $\{O_i\}$ (e.g., Tokovinin 1992; Hogeveen 1992; Ducati et al. 2011). The comparison between the expected distribution and the observed sample is usually done by comparing histograms, not a very powerful approach, which does not allow statistical derivation of the best parameter(s) of the MRD and its (their) confidence intervals.

In previous studies, the observable used was the reduced mass function, y , obtained by dividing the mass function by the mass of the primary star, but see Lucy & Ricco (1979); Boffin (2010, 2015), who promoted the use of a logarithm of the observable instead. However, we will show that the expected distributions of both y and $\log y$ for very different MRDs are quite similar, respectively, turning the derivation of the true MRD quite difficult.

Here we present a novel algorithm to solve the problem, which consists of four parts. First, we introduce a new observable, S , which we coin the ‘modified mass function’, that is derived for each SB1. We then show that the shape of the distribution of the obtained S for a binary sample is similar to that of the underlying MRD of the population. Even more importantly, different MRDs result in different S -distributions.

Second, we suggest to compare the expected distribution of S with the observed sample by deriving the *likelihood* of the observed set of $\{S_i\}$, given the assumed MRD (see also Tokovinin 1992). We can then find the parameters of the MRD that maximize the likelihood of observing the sample, using MCMC approach, for example.

Third, we suggest to express the unknown MRD by a linear combination of a basis of functions, with some unknown coefficients. We then search for the coefficients that maximizes the likelihood of the observed sample.

Fourth, following Mazeh & Goldberg (1992) we show how to account for the undetected binaries that have an RV amplitude below a certain threshold. Without the correction, this observational bias suppresses the derived MRD for low mass ratios.

Section 2 introduces the modified mass function, Section 3 details the search for the best set of parameters using MCMC process, and suggests two sets of functions, and Section 4 brings two simulated examples which demonstrate

that the algorithm works well. Section 5 presents our correction function, and Section 6 briefly summaries this work and lays out possible further refinements of the algorithm. In the next papers we apply the algorithm to various SB1 samples.

2 THE MODIFIED MASS FUNCTION

The mass-ratio of a binary system is defined as $q \equiv m_2/m_1$, where m_1 , m_2 are the stellar masses of the primary and secondary, respectively. For an SB1, only the spectrum of m_1 is seen in the spectrum of the system, and therefore only the primary RVs are obtained. When enough measurements are secured an orbital solution is derived, yielding the orbital period, P , eccentricity, e , and primary RV semi-amplitude, K_1 . The binary mass function is defined as

$$f(m_1) \equiv \frac{PK_1^3}{2\pi G} (1-e^2)^{3/2} = m_1 \frac{q^3}{(1+q)^2} \sin^3 i, \quad (1)$$

where i is the orbital inclination. An estimate of m_1 is often available from the binary spectra and can be factored out, leaving a ‘reduced mass function’, y , with only two unknown parameters, q and i :

$$y \equiv \frac{f(m_1)}{m_1} = \frac{q^3}{(1+q)^2} \sin^3 i. \quad (2)$$

Henceforth, we assume that the primary is also the more massive star in the binary system, namely $0 < q \leq 1$. Under this assumption the reduced mass function becomes bounded as well, $0 < y \leq 0.25$. The relation between q , y and i is plotted in Figure 1. We choose to work in the $(1 - \cos i, q)$ plane, as the distribution of $1 - \cos i$ is uniform for random orientation of the orbits. The plot shows the possible values of q for a binary with $y = 10^{-2}$. The gray area in the plot shows all the possible cases with $y \leq 10^{-2}$.

Notably, each value of y is associated with a minimal possible q value, that can be determined by setting the inclination angle i in equation (2) to be 90° . This q minimum, \mathcal{Q}_y , is the only real root of the polynomial $P_y(q)$,

$$P_y(\mathcal{Q}_y) = y^{-1} \mathcal{Q}_y^3 - \mathcal{Q}_y^2 - 2\mathcal{Q}_y - 1 = 0, \quad (3)$$

for which an explicit expression was given by Heacox (1995) (see also equation (A3)). That value, 0.25 for $y = 10^{-2}$, is plotted as a red point in the diagram.

Previous techniques used the observable y or $\log y$ as tools for deriving the MRD. For the direct method one needs to obtain the probability density function (PDF) of y , f_y , or $f_{\log y}$, given the PDF of the MRD, f_q . To obtain $f_y(y; f_q)$ one has to calculate the probability to get a value between y and $y+dy$ over the parameter space of Figure 1, given $f_q(q)$. This is done in Appendix A.

We seek a transformation $S = \mathbb{S}(y)$ such that significant functional properties of the MRD, f_q , will be qualitatively demonstrated by its resulting PDF, f_S . This results in three requirements. First, a uniform f_q should yield a uniform f_S . Second, the transformation \mathbb{S} is required to be strictly increasing and continuous. Finally, for f_S to be comparable with f_q , the range of \mathbb{S} is required to be the $[0, 1]$ interval.

These requirements are uniquely met by the cumulative distribution function (CDF) of y , *assuming a uniform distribution of q* . For example, $\mathbb{S}(y = 10^{-2})$ is simply the gray

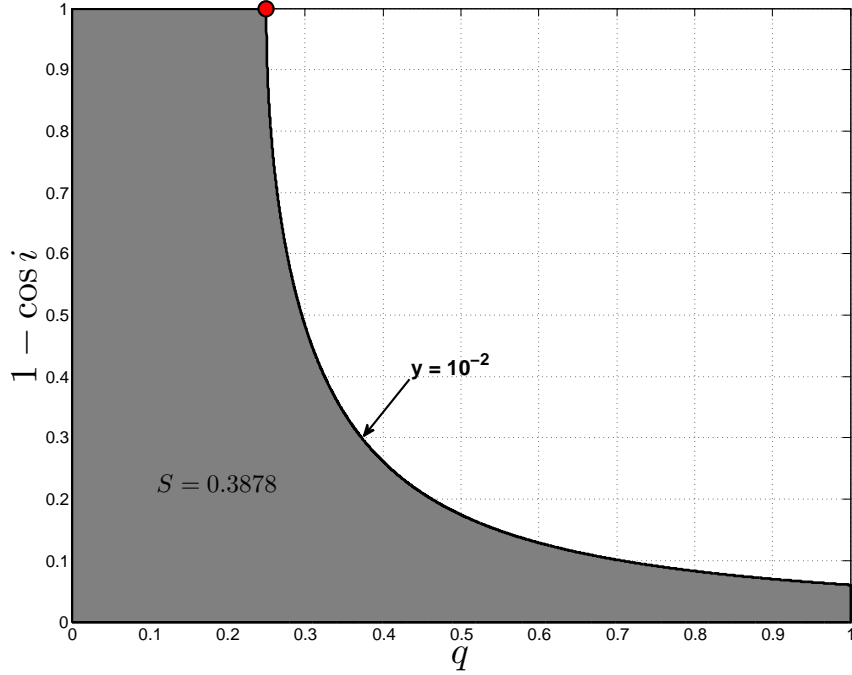


Figure 1. The $(1 - \cos i, q)$ parameter space, with an SB1 with $y = 10^{-2}$. Gray area—the corresponding S value. Red dot marks the minimum value of $q - \mathcal{Q}_y$, of 0.25.

area of Figure 1 for $y = 10^{-2}$. The area can be written as the integral

$$S = \mathbb{S}(y) \equiv 1 - \int_{\mathcal{Q}_y}^1 \sqrt{1 - y^{2/3} (1 + q)^{4/3} q^{-2}} dq, \quad (4)$$

where the integrand is the height above the curve of Figure 1. The relation between S , hereafter named the ‘modified mass function’, and y is demonstrated in Figure 2.

The modified mass function, by its definition, resembles to a copula (e.g., Nelsen 2013). While copulas are widely used in many fields, especially in quantitative finance, its astrophysical applications are rare (Scherrer et al. 2010, for example). Detailed derivation of \mathbb{S} appears in Appendix B.

2.1 Distribution of the modified mass function

To derive the PDF of S we note that S is defined as a function of y , and therefore

$$f_S(S; f_q) = f_y(y(S); f_q) \cdot \left| \frac{dy}{dS} \right|, \quad (5)$$

where $y(S)$ is the inverse of \mathbb{S} . Since the modified mass function, S , is by definition the CDF of y for a uniform MRD, the last factor in the equation above is

$$\left| \frac{dy}{dS} \right| = \frac{1}{f_y(y(S); 1)}. \quad (6)$$

We therefore get

$$f_S(S; f_q) = f_y(y(S); f_q) \cdot \left| \frac{dy}{dS} \right| = \frac{f_y(y(S); f_q)}{f_y(y(S); 1)}. \quad (7)$$

An explicit expression for f_y is developed in Appendix A, and shown in equation (A7). Inserting the two expressions—the PDF of y for the actual MRD and for flat distribution, we finally get

$$f_S(S; f_q) = \int_{\mathcal{Q}_{y(S)}}^1 f_q(q) \mathbb{K}(y(S), q) dq \Big/ \int_{\mathcal{Q}_{y(S)}}^1 \mathbb{K}(y(S), q) dq, \quad (8)$$

where

$$\mathbb{K}(y, q) = \frac{(1 + q)^{4/3}}{3y^{1/3} q \sqrt{q^2 - y^{2/3} (1 + q)^{4/3}}}, \quad (9)$$

(see Appendix A). Equation (8) is effectively a weighted average of f_q for a given S value, taken over the allowed q range, $[\mathcal{Q}_{y(S)}, 1]$, and weighted by the assumed distribution of isotropic inclination angles.

Figure 3 shows the derived f_y and f_S for three different simple f_q functions, demonstrating how, unlike f_y or $f_{\log y}$, f_S captures the shape of the underlying MRD, f_q .

3 DIRECT DERIVATION OF THE MRD

3.1 Likelihood derivation of the MRD

Let us assume that the MRD is characterized by a set of parameters $\mathbf{c} = \{c_k\}$. This could be, for example, a Gaussian distribution $f_q \propto \exp(-(q - c_1)^2 / 2c_2^2)$, a power-law distribution $f_q \propto q^{c_1}$, a flat distribution between $c_1 = q_{\min}$ and $c_2 = q_{\max}$, and alike, or any combination of the above. Using equation (8), we transform the $f_q(q; \mathbf{c})$ into $f_S(S; \mathbf{c})$, which has the same set of parameters $\{c_k\}$.

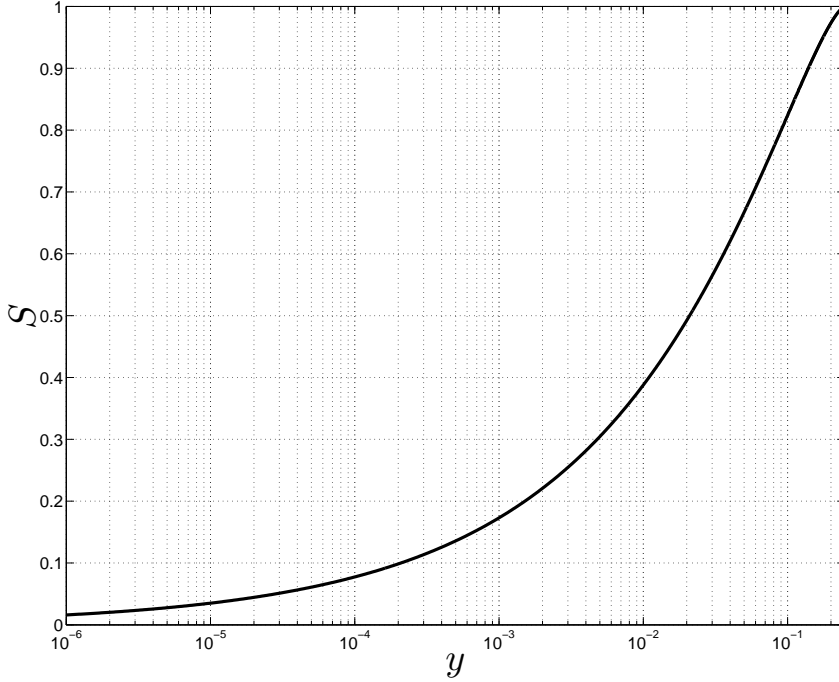


Figure 2. Modified mass function S as a function of the reduced mass function y .

We wish to find the values of the c_k 's that best match the given sample of observed SB1, with a set of $\{y_i\}$ that we transfer via equation (4) to the corresponding set of $\{S_i\}$. The search is done by maximizing the log-likelihood of \mathbf{c} ,

$$\log \mathcal{L}(\mathbf{c} | \{S_i\}), \quad (10)$$

given $\{S_i\}$. The core of the algorithm is the search for the best MRD in the S domain. Since the fitted c_k values are shared by both f_S and f_q , it is clear that by fitting f_S one readily derives its underlying f_q .

In practice, examples brought in this work were analyzed with the emcee ensemble sampler (Goodman & Weare 2010; Foreman-Mackey et al. 2013). Each step in the generated chain yields a set of values for the c_k 's, from which the MRD, f_q , is derived over a dense set of pre-determined $\{q_j\}$. The chain yields *a posteriori* distributions for each $\{f_q(q_j)\}$. We use these distributions to derive the median $\{\hat{f}_q(q_j)\}$ and their 1σ confidence intervals $\{\hat{\delta}(q_j)\}$ to finally yield

$$\hat{f}_q(q) \pm \hat{\delta}(q). \quad (11)$$

3.2 Expansion of MRD by a set of basis functions

Likelihood derivation of the MRD requires a predetermined functional model, whose parameters are searched to fit best the observed set of $\{S_i\}$. It is therefore desirable to use models that can span a broad class of functions, thus avoiding *a priori* assumptions about the functional shape of the MRD. This can be achieved by approximating f_q with a set of basis functions,

$$f_q(q) = \sum_k c_k \phi_k(q), \quad (12)$$

where $\phi_k(q)$ is the k -th function and c_k is its corresponding coefficient.

For each basis function we derive its corresponding function in the S plane, denoted $\tilde{\phi}_k(S)$, through equation (8),

$$\tilde{\phi}_k(S) \equiv f_S(S; \phi_k). \quad (13)$$

The linearity of equation (8) links the expansion of f_S to that of f_q via the modified functions, namely

$$f_S(S; f_q) = \sum_k c_k \tilde{\phi}_k(S), \quad (14)$$

where c_k is the k -th coefficient of the f_q series expansion. In this case, the parameterized probability density takes a simple form

$$f_S(S_i | \mathbf{c}) = \sum_k \tilde{\phi}_k(S_i) \cdot c_k \equiv \sum_k M_{ik} c_k, \quad (15)$$

where M_{ik} is the value of $\tilde{\phi}_k$ at S_i . This can be written in a matrix form

$$\mathbf{f}_S(S_i | \mathbf{c}) = \mathbf{M} \cdot \mathbf{c}, \quad (16)$$

where \mathbf{M} is the M_{ik} design matrix.

The design matrix \mathbf{M} can be calculated given the sample $\{S_i\}$, the basis $\{\phi_k(q)\}$ and its corresponding $\{\tilde{\phi}_k\}$. The log-likelihood in terms of \mathbf{M} is

$$\log \mathcal{L}(\mathbf{c} | \{S_i\}) = \sum_i \log \left(\sum_k M_{ik} c_k \right), \quad (17)$$

according to which the best \mathbf{c} can be found.

In the next subsections we suggest two possible sets of basis functions—the shifted Legendre polynomials and the boxcar functions. The two have complementary properties

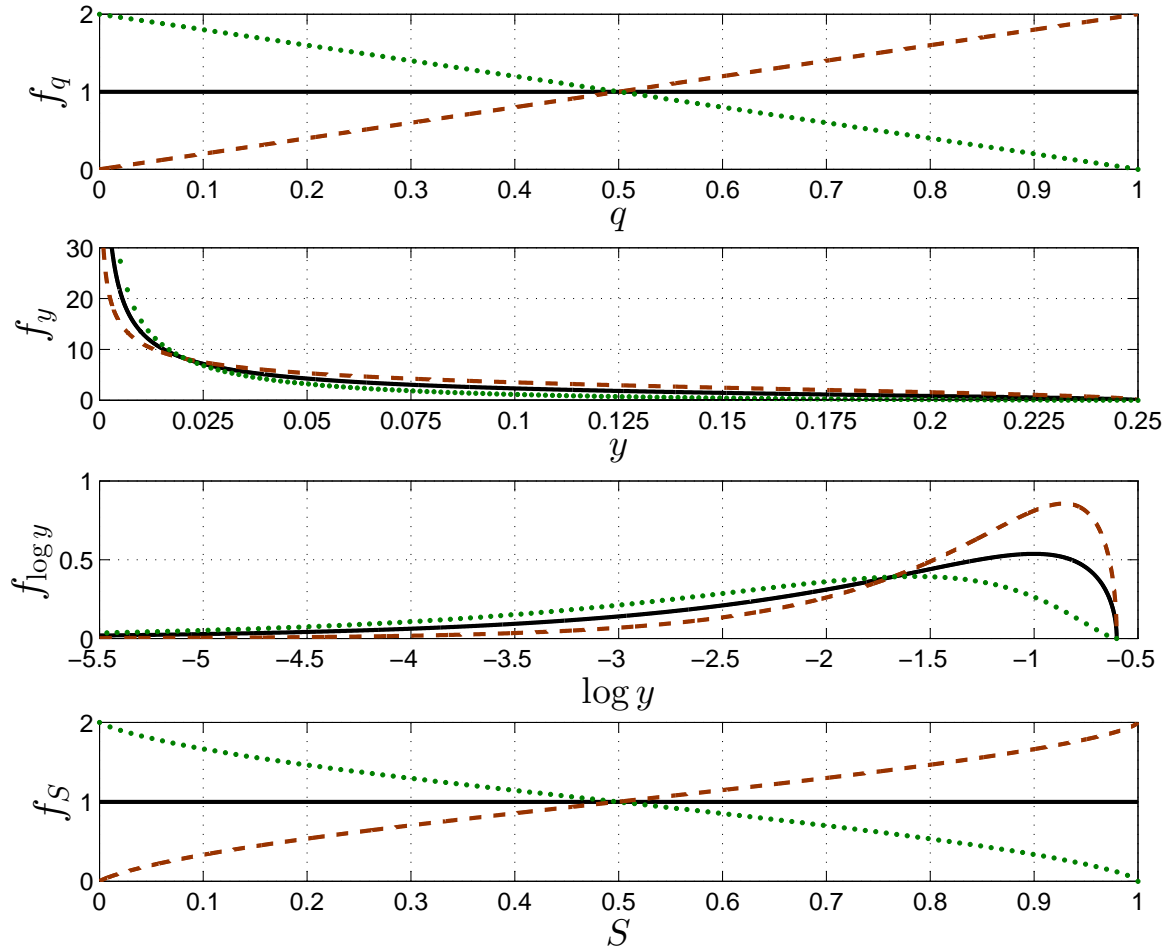


Figure 3. Three distributions of q and their corresponding y , $\log y$ and S distributions. Top panel: Uniform (black line), linearly increasing (brown dashed line) and decreasing (green dotted line) distributions of q . The three lower panels show the corresponding y , $\log y$ and S distributions, with the same color and shape lines.

in terms of smoothness and locality. Obviously, other possibilities, such as harmonic functions or power series, can be considered and implemented in a similar manner.

3.2.1 Shifted Legendre polynomials

A possible basis is, for example, the shifted Legendre polynomials, $\{P_k\}$:

$$\begin{aligned} P_0(x) &= 1, \\ P_1(x) &= 2x - 1, \\ P_2(x) &= 6x^2 - 6x + 1, \\ P_3(x) &= 20x^3 - 30x^2 + 12x - 1, \\ P_4(x) &= 70x^4 - 140x^3 + 90x^2 - 20x + 1. \\ &\vdots \end{aligned} \quad (18)$$

The first four $P_k(q)$, $P_0 - P_3$, are plotted in Figure 4, together with their corresponding modified functions $\tilde{P}_k(S)$.

The shifted Legendre polynomials have the property $\int_0^1 P_k(x) dx = \delta_{k0}$. This makes them suitable as a set of basis function for any PDF, as the integral of any combination of them over the range $[0,1]$ is unity, as long as $c_0 = 1$.

3.2.2 Boxcar functions

Another basis is the set of boxcar functions, $\{\Pi_{N,k}(x), k = 1, \dots, N\}$, that are simple unit pulses of the form

$$\Pi_{N,k}(x) = \begin{cases} 1 & \text{if } \frac{k-1}{N} \leq x \leq \frac{k}{N}, \\ 0 & \text{else,} \end{cases} \quad (19)$$

spanning the histogram-like models. The corresponding modified functions are derived through equation (8).

3.3 Starting point of the MCMC

In any MCMC search, it is important to start the chain not too far from the global maximum of the log-likelihood. Our starting point relies on the histogram of observed $\{S_i\}$. For the boxcar basis the starting point is taken as the normalized number of counts in the S histogram bins, whereas the starting point of the Legendre polynomial set was derived by a simple linear least squares fit to the histogram bins (see Barlow 1989).

To choose the number of bins, N_{bin} , for the histogram

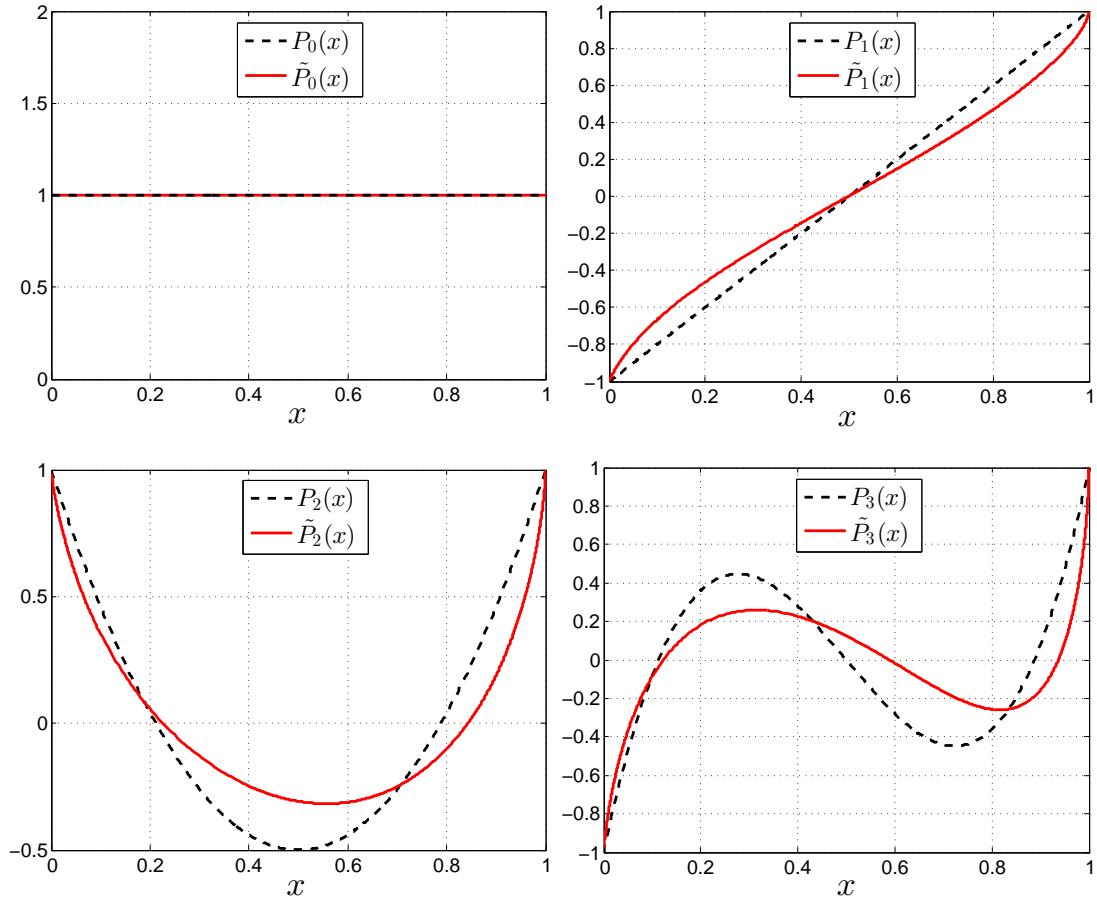


Figure 4. First four shifted Legendre polynomials (dashed black) and their corresponding modified functions (solid red).

we use the Rice rule (Terrell & Scott 1985),

$$N_{bin} = \lceil \sqrt[3]{2n} \rceil, \quad (20)$$

where n is the size of the observed sample.

4 TESTING THE ALGORITHM

In order to test our algorithm, and the two bases presented above in particular, we ran numerous simulations, two of which are presented here. In each numerical experiment we assumed an underlying MRD and prepared a simulated SB1 sample, drawing at random values for the mass ratio and inclination of each binary. We then derived the S value for each binary and applied our algorithm to the sample of modified mass functions twice, using in each time one of our two bases.

In all our simulations we were able to retrieve the correct shape of the underlying MRD, with each of the two bases.

Here we present two simulations, one (Figure 5) with an MRD composed of a fourth-degree polynomial, $f_q(q) \propto 25(2q-1)^4 + 4$, that peaks at $q=0$ and $q=1$, and the other (Figure 6) composed of a Gaussian with a mean at $q=0.2$

and a standard deviation of 0.15 (77% of the population) together with a flat distribution in the range $q=[0,1]$ (23%). Since typically the number of SBs in modern spectroscopic surveys is on the order of 100 (Goldberg et al. 2003, analyzed 129 SBs, for example), we chose the size of the simulated sample to be 100 SB1 systems in both examples.

The best MRD model and its uncertainty were derived by calculating the median and scatter of the values obtained for each q along the MCMC run, as described in subsection 3.1. The top panels of Figures 5 and 6 show the MRD used and the mass-ratio histogram of the simulated sample, while the bottom panels present the MRDs derived with a basis of seven boxcar functions and with the first five shifted Legendre polynomials.

An alternative method of deriving an explicit expression for the best fitting model is by taking median value of each parameter obtained along the chain. For example, the fitted MRD, in terms of the shifted Legendre polynomials given in equation (18), for the two experiments presented above in this section are

$$\begin{aligned} \hat{f}_1(q) &= 1.22P_4(q) - 0.35P_3(q) + 1.54P_2(q) + 0.11P_1(q) + P_0(q), \\ \hat{f}_2(q) &= -0.65P_4(q) + 0.99P_3(q) + 0.14P_2(q) - 1.22P_1(q) + P_0(q), \end{aligned}$$

where \hat{f}_1 and \hat{f}_2 are the fitted models for the simulations presented in Figures 5 and 6, respectively. By gathering terms of the same power in q , the derived MRDs become

$$\begin{aligned}\hat{f}_1(q) &= 85.6q^4 - 178.2q^3 + 129.8q^2 - 37.7q + 4.0, \\ \hat{f}_2(q) &= -45.7q^4 + 111.0q^3 - 87.4q^2 + 21.6q + 0.7.\end{aligned}$$

Differences between the MRDs derived by the two methods are found to be $\lesssim \sigma/5$.

The two examples demonstrate the power of our algorithm, as the derived MRDs are very close to the underlying functions, even though the algorithm was applied without any assumption on the shape of the MRD.

5 ACCOUNTING FOR AN OBSERVATIONAL DETECTION THRESHOLD

Samples of observed spectroscopic binaries are subjected to many observational biases. An obvious one (e.g., Mazeh & Goldberg 1992; Tokovinin 1992) is the detection threshold—RV surveys can identify SB systems only if their RV amplitude is large enough. The impact of such a selection effect becomes increasingly significant for small values of q , causing the derived \hat{f}_q at small q values to be underestimated. In this section we describe our way to account for this observational bias, following the approach of Mazeh & Goldberg (1992).

To model this effect we assume that only (and all) binaries with RV amplitude larger than some K_{\min} are detected. Therefore, for each q and m_1 there exists the longest orbital period that can be detected:

$$P_{\max} = \left(\frac{m_1}{m_{\odot}}\right) \left(\frac{K_{\min}}{1 \text{ km/s}}\right)^{-3} \frac{q^3}{(1+q)^2} 9.625 \cdot 10^6 \text{ d}, \quad (21)$$

where the orbits are assumed to be circular. For periods shorter than P_{\max} the detectability depends on the inclination angle and therefore only a fraction of the population of binaries are detectable. We define the detection function, D , which is the fraction of detected binaries out of all systems with identical P , m_1 and q . The detection function is the probability of a system to have an inclination such that its observed RV semi-amplitude will be larger than the detection threshold,

$$D = \begin{cases} \sqrt{1 - 2.21 \cdot 10^{-5} K_{\min}^2 \frac{P^{2/3}}{m_1^{2/3}} \frac{(1+q)^{4/3}}{q^2}} & \text{if } P < P_{\max}, \\ 0 & \text{else,} \end{cases} \quad (22)$$

where P is in days, m_1 is in solar mass and K_{\min} is in km/s.

Let us further assume that the primary stars in the sample are of nearly identical mass, \bar{m} , and that the distribution of the orbital period, f_P , is independent of q . The fraction of detected systems with some specific q is composed of the probability that both the period and the inclination allow a detection, namely

$$\bar{D}(q) = \int_{P_1}^{P_2} D(q, P, \bar{m}, K_{\min}) f_P(P) dP, \quad (23)$$

where P_1 and P_2 are the shortest and longest periods of the population, respectively.

The derived \hat{f}_q can now be corrected by the detection function, namely

$$\hat{h}_q(q) = \frac{\hat{f}_q(q)}{\bar{D}(q)}, \quad (24)$$

where $\hat{h}_q(q)$ is the unbiased distribution of q . This time the corrected function has to be normalized in order to be used as a PDF. In the case of a boxcar fit, the correction factor of each bin is taken according to its value at the bin's center. Notably, for very small mass ratios the correction factor, $1/\bar{D}(q)$, becomes very large and consequently uncertain. It is therefore advised to cautiously address only a domain where the correction factor is a small number, say, $1/\bar{D}(q) \lesssim 2$.

Again, to test the correcting part of the algorithm we ran numerous simulations, one of which is presented in Figure 7. We used here the same population as in Figure 5, but now with $1M_{\odot}$ primary for each binary, orbital periods with log-uniform distribution between 1 to 10^3 days, and a detection threshold of $K_{\min} = 3$ km/s, which caused 22 simulated binaries not to be detected. A histogram of the detected and missed binaries is plotted in the top panel of Figure 7. As can be seen in the figure, most of the missed binaries had low mass ratio, as expected. The lower panel shows the uncorrected and corrected distributions. The uncorrected MRD suffers from serious suppression of its lower part, while the correction succeeded to produce the correct underlying MRD. As expected, for small mass ratios, $q \lesssim 0.05$, the correction factor ($1/\bar{D}(q)$) became large, and therefore, we refrained from obtaining the corrected function for this range of q 's.

Another way to correct for the undetected binaries, not presented here, is to apply the derived $\bar{D}(q)$ factor to the base functions, and use these corrected functions along the MCMC fitting. One then constructs the true MRD by using the uncorrected base functions with the parameters obtained with the MCMC.

6 CONCLUSIONS

We have presented here a novel *direct* algorithm to derive the mass-ratio distribution (MRD) of short-period binaries from an observed SB1 sample. The algorithm considers a parameterized family of MRDs and finds the set of parameters that best fits the observed sample.

The algorithm consists of four parts. First, we define a new observable, the modified mass function, S , derived for each SB1 in the sample. We show that the distribution of the modified mass function of an SB1 sample follows the shape of the underlying MRD, turning the use of the modified mass function more advantageous than the previously used mass function, reduced mass function or the reduced mass function logarithm. Second, given an assumed MRD, we derive the likelihood of obtaining the observed sample of SB1s with the derived modified mass functions. Maximizing this likelihood by an MCMC search enables the algorithm to find the best parameters of the underlying MRD. Third, we suggest to express the unknown MRD by a basis of functions with some unknown coefficients that linearly span the space of possible MRDs. We suggest two such bases. Fourth, we have shown how to account for the undetected systems that have an RV amplitude below a certain threshold. The

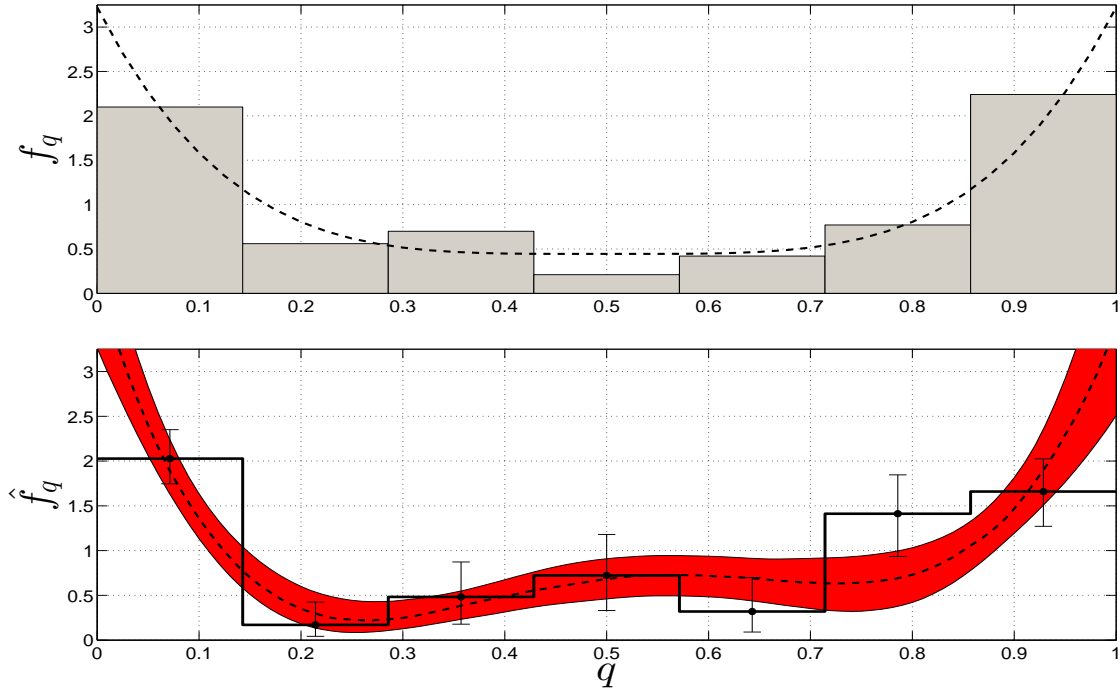


Figure 5. Derivation of MRD from a simulation 100 SB1 sample. Top: Simulated sample of 100 SB1s, with random orientations, using as an MRD (dashed black line) a fourth-degree polynomial, $f_q(q) \propto 25(2q-1)^4 + 4$, that peaks at $q=0$ and $q=1$. The specific drawn sample is presented by a seven-bin histogram. Bottom: Two independent derived MRDs, one uses the first *five* shifted Legendre polynomials as a basis (dashed black line) and the other one the boxcar basis of seven bins (thick black line). Each derived MRD is associated with an error for each value of q (see text).

correction is calculated per mass ratio and therefore can be applied to the derived MRD. Without the correction, this observational bias suppresses the derived MRD for low mass ratios. Numerous simulations show that the algorithm works with either of the two bases.

The algorithm is based on three simplifications. We consider here only circular orbits, we ignore the double-lined binaries, and we assume there are no uncertainties associated with the y 's and therefore with the S 's. With the present layout, it is straightforward to generalize the algorithm to include eccentric orbits and uncertainties in the S 's. On the other hand, ignoring the extra information about the known mass ratio of the SB2s (e.g., Mazeh et al. 2003; Prato 2007; Fernandez et al. 2017) is an obvious drawback. A further development of the algorithm to use the SB2 information is planned for a further publication. At present, the algorithm treats those systems as SB1s.

The detection threshold correction presented here depends on the orbital period distribution of the binary population and on the assumption that the MRD does not depend on the binary period (see discussion by Moe & Di Stefano 2017, which put this assumption into question for O- and B-type stars). These two assumptions are inherent to any correction algorithm, as the RV amplitude does depend on the mass ratio and the orbital period. The simulations showed that the correction succeeded to produce the correct MRD for low mass ratios.

The correction is based on a simplistic conception of the detection threshold. In reality, the observational bias

does not act as a stiff threshold, but instead the detection probability of a binary is a continuous monotonic increasing function of its amplitude, which depends on the period, determined by the time stamp of the RV observations. However, it is quite easy to adopt the algorithm to any detection sensitivity through equations (22) and (23), by which one can derive a more sophisticated correction for any value of mass ratio. Needless to say, any derivation of the mass ratio distribution can be based only a sample that was obtained by a complete systematic survey that searches for spectroscopic binaries with known detection thresholds, so that the corrections can be derived and applied to the observed sample.

Obviously, the correction procedure introduces additional errors to the derived MRD, due to an inexact period distribution and inaccurate detection threshold used. Therefore, the correction becomes less valuable for low mass ratios, a range for which we have small number of systems and the correction factor becomes large. In the simulated case presented above, for example, we refrained from plotting the corrected MRD for mass ratio smaller than 0.05. The exact limit depends on the specific SB1 sample.

In the next paper of this series (Shahaf et al., in preparation) we apply the algorithm to a few samples published in the literature, in particular those of Mazeh et al. (2003), Fisher et al. (2005), Prato (2007), Mermilliod et al. (2007) (see also North 2014; Van der Saelmen et al. 2017) and Tal-Or et al. (2015).

Furthermore, we anticipate in the near future extremely

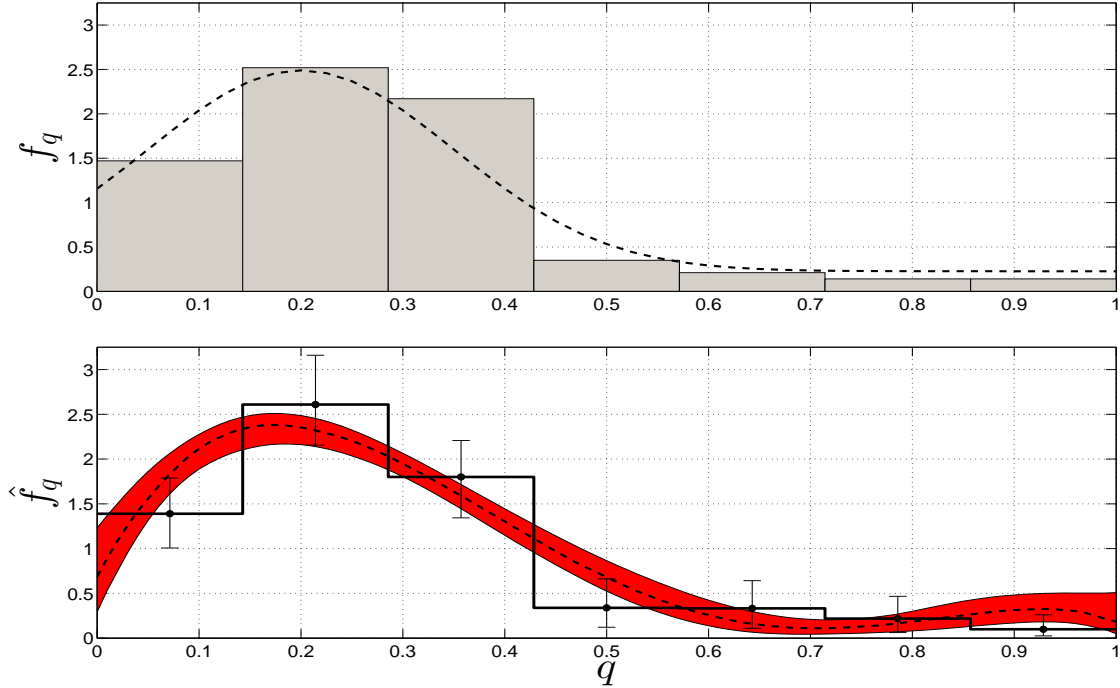


Figure 6. Derivation of MRD from a simulation 100 SB1 sample. The simulated MRD is composed of a Gaussian with a mean at $q=0.2$ and width of 0.15 (77% of the population) and a flat part in the range $q=[0,1]$ (23%). The simulated sample and the two derived MRDs are plotted as in Figure 5.

large new samples of SBs coming from the APOGEE¹ and the Gaia² projects. The release of the Gaia distances will enable us to better estimate the primary masses of these samples, a key element in the derivation of the reduced and modified mass function. The new algorithm will be ready for these large samples to determine the MRD of spectroscopic binaries. In addition, we anticipate two additional large samples—eclipsing binaries from large photometric data bases (see, for example Mazeh et al. 2006; Mowlavi et al. 2017, for the analysis of the OGLE LMC binaries), and astrometric binaries from Gaia, exploring the binaries with very short and very long period range. The new samples will finally give us the full picture of the different binary populations.

ACKNOWLEDGMENTS

We are indebted to the referee for the thorough reading of the manuscript and very helpful comments. We thank Shay Zucker for the insightful discussions. We acknowledge support from the Israel Science Foundation (grant No. 1423/11) and the Israeli Centers of Research Excellence (I-CORE, grant No. 1829/12).

¹ <http://www.sdss3.org/surveys/apogee.php>

² <http://sci.esa.int/gaia/>

REFERENCES

- Barlow R., 1989, Least Squares, in Statistics. A guide to the use of statistical methods in the physical sciences, pp. 105-115
- Bate M. R., Bonnell I. A., 1997, *MNRAS*, **285**, 33
- Benacquista M. J., Downing J. M. B., 2013, *Living Reviews in Relativity*, **16**, 4
- Boffin H. M. J., 2010, *A&A*, **524**, A14
- Boffin H. M. J., 2015, *A&A*, **575**, L13
- Curé M., Rial D. F., Cassetti J., Christen A., Boffin H. M. J., 2015, *A&A*, **573**, A86
- Ducati J. R., Penteado E. M., Turcati R., 2011, *A&A*, **525**, A26
- Duquennoy A., Mayor M., 1991, *A&A*, **248**, 485
- Fernandez M. A., et al., 2017, preprint, ([arXiv:1706.01161](https://arxiv.org/abs/1706.01161))
- Fisher J., Schröder K.-P., Smith R. C., 2005, *MNRAS*, **361**, 495
- Foreman-Mackey D., et al., 2013, emcee: The MCMC Hammer, *Astrophysics Source Code Library* (ascl:1303.002)
- Goldberg D., Mazeh T., Latham D. W., 2003, *ApJ*, **591**, 397
- Goodman J., Weare J., 2010, *Communications in Applied Mathematics and Computational Science*, Vol. **5**, 65
- Grether D., Lineweaver C. H., 2006, *ApJ*, **640**, 1051
- Heacox W. D., 1995, *AJ*, **109**, 2670
- Hogeveen S. J., 1992, *Ap&SS*, **196**, 299
- Hut P., et al., 1992, *PASP*, **104**, 981
- Kouwenhoven M. B. N., Brown A. G. A., Goodwin S. P., Portegies Zwart S. F., Kaper L., 2009, *A&A*, **493**, 979
- Lucy L. B., 1974, *AJ*, **79**, 745
- Lucy L. B., Ricco E., 1979, *AJ*, **84**, 401
- Mazeh T., Goldberg D., 1992, *ApJ*, **394**, 592
- Mazeh T., Simon M., Prato L., Markus B., Zucker S., 2003, *ApJ*, **599**, 1344
- Mazeh T., Tamuz O., North P., 2006, *MNRAS*, **367**, 1531
- Mermilliod J.-C., Andersen J., Latham D. W., Mayor M., 2007,

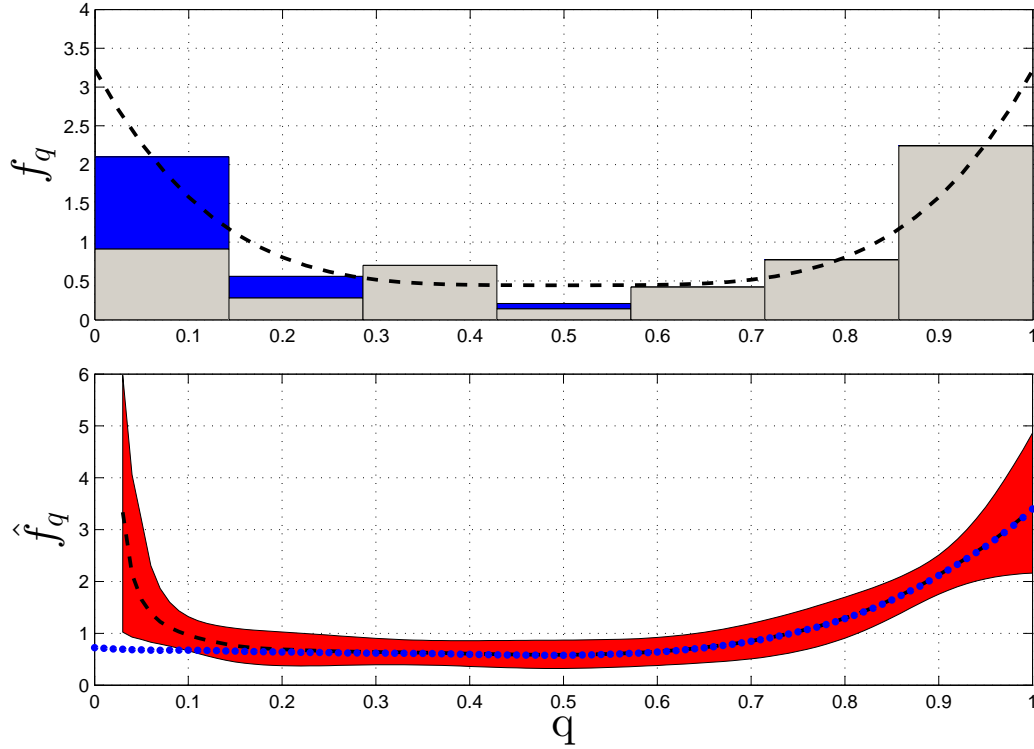


Figure 7. MRD Derivation from a simulated SB1 sample with a detection threshold of $K_{\min} = 3$ km/s. Top: Simulated sample of 100 SB1s with random orientations, using an MRD (dashed black line) that peaks at $q=0$ and $q=1$. The specific drawn sample is presented by a seven (gray) bin histogram (see Figure 7). Because of the detection threshold, 22 systems (light blue) upper bins, were not detected. Bottom: Derived MRD (dotted line), using the first *five* shifted Legendre polynomials as a basis, together with the corrected MRD (dashed line) and its confidence 1σ range (see text).

[A&A, 473, 829](#)

Moe M., Di Stefano R., 2017, [ApJS, 230, 15](#)

Mowlavi N., et al., 2017, preprint, ([arXiv:1703.10597](#))

Nelsen R., 2013, An Introduction to Copulas. Lecture Notes in Statistics, Springer New York, <https://books.google.co.il/books?id=EqbzBwAAQBAJ>

North P., 2014, in Mathys G., Griffin E. R., Kochukhov O., Monier R., Wahlgren G. M., eds, Putting A Stars into Context: Evolution, Environment, and Related Stars. pp 63–71 ([arXiv:1309.7636](#))

Prato L., 2007, [ApJ, 657, 338](#)

Raghavan D., et al., 2010, [ApJS, 190, 1](#)

Satsuka T., Tsuribe T., Tanaka S., Nagamine K., 2017, [MNRAS, 465, 986](#)

Scherrer R. J., Berlind A. A., Mao Q., McBride C. K., 2010, [ApJ, 708, L9](#)

Tal-Or L., Faigler S., Mazeh T., 2015, [A&A, 580, A21](#)

Terrell G. R., Scott D. W., 1985, [Journal of the American Statistical Association, 80, 209](#)

Tokovinin A. A., 1992, [A&A, 256, 121](#)

Tokovinin A. A., 2000, [A&A, 360, 997](#)

Toonen S., Nelemans G., Portegies Zwart S., 2012, [A&A, 546, A70](#)

Trimble V., 1990, [MNRAS, 242, 79](#)

Van der Swaelmen M., Boffin H. M. J., Jorissen A., Van Eck S., 2017, [A&A, 597, A68](#)

Yungelson L. R., Kuranov A. G., 2017, [MNRAS, 464, 1607](#)

APPENDIX A: DISTRIBUTION OF THE REDUCED MASS FUNCTION

The mass-ratio of a binary system is $q \equiv m_2/m_1$, where m_1 , m_2 are the stellar masses of the primary and secondary, respectively. The reduced mass function, y , is

$$y = \frac{q^3}{(1+q)^2} \sin^3 i. \quad (\text{A1})$$

where i is the inclination. Notably, each value of y is associated with a minimal possible q value, that can be determined by setting the inclination angle i to be 90° . This q minimum, denoted \mathcal{Q}_y , is the only real root of the polynomial $P_y(q)$,

$$P_y(\mathcal{Q}_y) = y^{-1} \mathcal{Q}_y^3 - \mathcal{Q}_y^2 - 2\mathcal{Q}_y - 1 = 0. \quad (\text{A2})$$

The explicit expression for \mathcal{Q}_y , as was given by Heacox (1995), is

$$\mathcal{Q}_y = h(y) + \frac{1}{h(y)} \left(\frac{2}{3}y + \frac{1}{9}y^2 \right) + \frac{1}{3}y, \quad (\text{A3})$$

where

$$h(y) = \left(\frac{1}{2}y + \frac{1}{3}y^2 + \frac{1}{27}y^3 + \frac{\sqrt{3}y}{18} \sqrt{(4y+27)} \right)^{1/3}. \quad (\text{A4})$$

A rigorous development of the y probability density function (PDF), f_y , for a sample of randomly oriented binaries has been previously presented by Heacox (1995). Nevertheless, an alternative geometrical derivation of it may be instructive in the context of this work.

We choose to work in the parameter plane of $(1 - \cos i, q)$, where $0 \leq q \leq 1$ and $0 \leq 1 - \cos i \leq 1$, as the distribution of $1 - \cos i$ is uniform for random orientation of the orbits. Equation (A1) implies that y values are uniquely associated with contours on that plane, as demonstrated in Figure A1. A specific system with some given $y \pm \delta y/2$ and $q \pm \delta q/2$ occupies an area on the parameter plane,

$$\delta A = \delta(1 - \cos i) \delta q \approx \left| \frac{\partial \cos i}{\partial y} \right| \delta y \delta q, \quad (\text{A5})$$

where by means of equation (A1), $\left| \frac{\partial \cos i}{\partial y} \right|$ is

$$\mathbb{K}(y, q) \equiv \left| \frac{\partial \cos i}{\partial y} \right| = \frac{(1+q)^{4/3}}{3y^{1/3} q \sqrt{q^2 - y^{2/3}(1+q)^{4/3}}}. \quad (\text{A6})$$

An example of δA assuming $0.0100 \leq y \leq 0.0101$, at $q = 0.3$, is given in Figure A1.

Since $1 - \cos i$ is uniformly distributed, the probability to draw a system with specific y and q values from a sample of randomly oriented binaries is $\sim f_q(q) \delta A$, where f_q is the sample's underlying MRD. Considering all possible values of q , taking δA to be infinitesimal and assuming $0 < q \leq 1$, f_y becomes

$$f_y(y; f_q) = \int_{\mathcal{Q}_y}^1 f_q(q) \cdot \mathbb{K}(y, q) dq. \quad (\text{A7})$$

Some attempts have been made to use the PDF of $\log(y)$, $f_{\log y}$, as a more informative representation of the data (e.g., Boffin 2010, 2015). In terms of equation (A7), $f_{\log y}$ is

$$f_{\log y}(u; f_q) \propto 10^u \cdot f_y(10^u; f_q). \quad (\text{A8})$$

APPENDIX B: DERIVATION OF THE MODIFIED MASS FUNCTION

The modified mass function, S , is required to be a strictly increasing continuous transformation of y , from $[0, 0.25]$ onto $[0, 1]$. Additionally, if the underlying MRD, f_q , is uniform—its resulting S distribution, f_S , is required to be uniform as well.

According to equation (2) $\cos i$ can be expressed in terms of y and q ,

$$\cos i(y, q) = \sqrt{1 - y^{2/3}(1+q)^{4/3}q^{-2}}. \quad (\text{B1})$$

The probability to observe a system at some $y' < y$ is provided by integrating over the surface bounded by the axis, a contour of $1 - \cos i(y, q)$ within the $(1 - \cos i, q)$ plane, namely

$$P(y' < y) = \int_A f_{(1-\cos i)} \cdot f_q dA. \quad (\text{B2})$$

Since $1 - \cos i$ is uniformly distributed,

$$P(y' < y) = \int_0^{\mathcal{Q}_y} f_q dq + \int_{\mathcal{Q}_y}^1 (1 - \cos i(y, q)) f_q dq. \quad (\text{B3})$$

The modified mass function is defined by taking equation (B3) with uniform MRD:

$$S = \mathbb{S}(y) \equiv 1 - \int_{\mathcal{Q}_y}^1 \sqrt{1 - y^{2/3}(1+q)^{4/3}q^{-2}} dq. \quad (\text{B4})$$

The transformation \mathbb{S} is by definition the CDF of y assuming a uniform MRD, therefore it obeys the requirements given at the beginning of this subsection.

\mathbb{S} is unique. Let \mathbb{T} and \mathbb{S} uphold the stated requirements. Since both are transformations of y , the probability density functions obey $f_S \left| \frac{dS}{dy} \right| = f_T \left| \frac{dT}{dy} \right|$. Specifically for uniform f_q , this relation becomes $\left| \frac{dS}{dy} \right| = \left| \frac{dT}{dy} \right|$. Since both are strictly increasing and continuous from $[0, 0.25]$ onto $[0, 1]$, $\mathbb{T} \equiv \mathbb{S}$.

This paper has been typeset from a $\text{\TeX}/\text{\LaTeX}$ file prepared by the author.

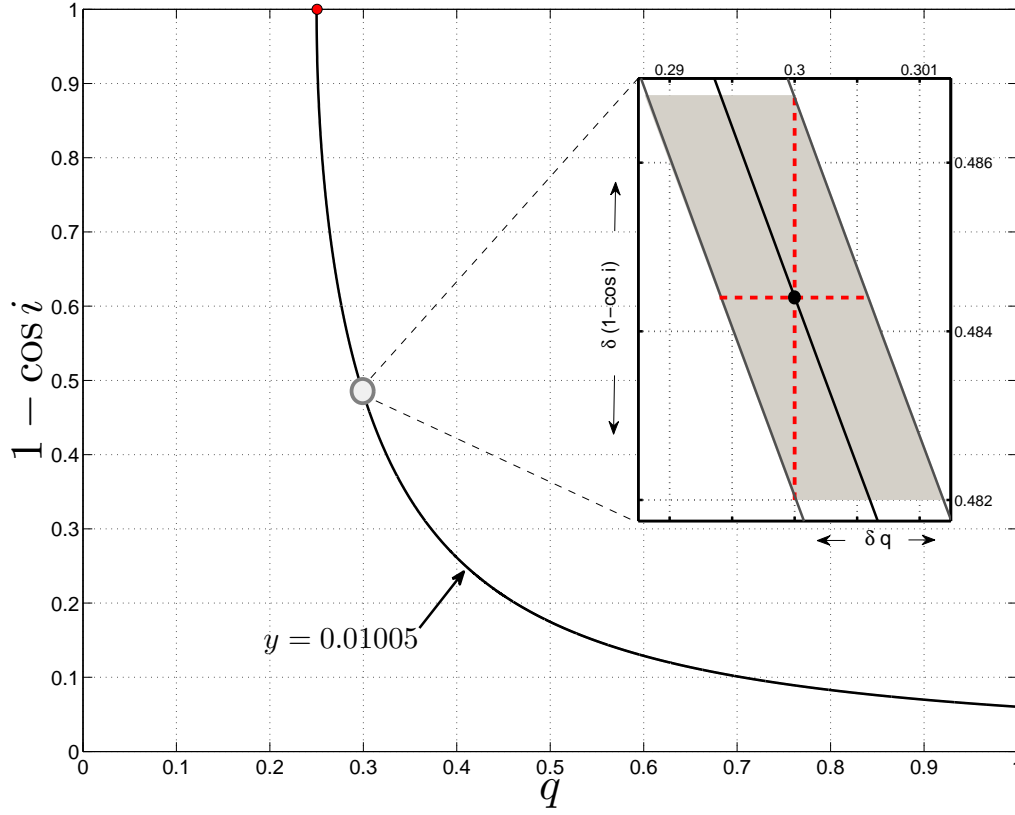


Figure A1. A contour of $y = 0.01005$ plotted in the $(1 - \cos i, q)$ plane. The red dot corresponds to the q minimum value of $y = 0.01005$. Gray circle locates the point where $q = 0.3$. The zoomed window shows the area bounded by $0.0100 \leq y \leq 0.0101$. The horizontal width of the parallelogram, δq , equals to 0.0012 (dashed red). The vertical height of the parallelogram, $\delta(1 - \cos i)$, equals to $\mathbb{K}(y, q) \times \delta y = 0.0047$ (dashed red).